



Calibrating the SAR SSH of Sentinel-3A and CryoSat-2 over the Corsica Facilities

Pascal Bonnefond, Olivier Laurain, Pierre Exertier, François Boy, Thierry Guinle, Nicolas Picot, Sylvie Labroue, Matthias Raynal, Craig Donlon, Pierre Féménias, et al.

► To cite this version:

Pascal Bonnefond, Olivier Laurain, Pierre Exertier, François Boy, Thierry Guinle, et al.. Calibrating the SAR SSH of Sentinel-3A and CryoSat-2 over the Corsica Facilities. *Remote Sensing*, 2018, 10 (1), 10.3390/rs10010092 . hal-01852691

HAL Id: hal-01852691

<https://hal.science/hal-01852691>

Submitted on 18 Dec 2020

HAL is a multi-disciplinary open access archive for the deposit and dissemination of scientific research documents, whether they are published or not. The documents may come from teaching and research institutions in France or abroad, or from public or private research centers.

L'archive ouverte pluridisciplinaire **HAL**, est destinée au dépôt et à la diffusion de documents scientifiques de niveau recherche, publiés ou non, émanant des établissements d'enseignement et de recherche français ou étrangers, des laboratoires publics ou privés.



Distributed under a Creative Commons Attribution - NoDerivatives 4.0 International License

Article

Calibrating the SAR SSH of Sentinel-3A and CryoSat-2 over the Corsica Facilities

Pascal Bonnefond ^{1,*}, Olivier Laurain ², Pierre Exertier ², François Boy ³, Thierry Guinle ³, Nicolas Picot ³, Sylvie Labroue ⁴, Matthias Raynal ⁴ , Craig Donlon ⁵, Pierre Féménias ⁶, Tommaso Parrinello ⁶ and Salvatore Dinardo ⁷

¹ SYRTE, Observatoire de Paris, PSL Research University, CNRS, Sorbonne Universités, UPMC University Paris 06, LNE, 75014 Paris, France

² Géoazur, Observatoire de la Côte d’Azur, 06905 Sophia-Antipolis CEDEX, France; Olivier.Laurain@oca.eu (O.L.); Pierre.Exertier@oca.eu (P.E.)

³ Centre National d’Etudes Spatiales (CNES), 31401 Toulouse CEDEX, France; Francois.Boy@cnes.fr (F.B.); Thierry.Guinle@cnes.fr (T.G.); Nicolas.Picot@cnes.fr (N.P.)

⁴ Collecte Localisation Satellites (CLS), 31520 Ramonville Saint-Agne, France; Sylvie.Labroue@cls.fr (S.L.); mraynal@cls.fr (M.R.)

⁵ European Space Agency/European Space Research and Technology Centre (ESA/ESTEC), 2201 AZ Noordwijk, The Netherlands; Craig.Donlon@esa.int

⁶ European Space Agency/European Space Research Institute (ESA/ESRIN), 00044 Frascati, Italy; Pierre.Femenias@esa.int (P.F.); Tommaso.Parrinello@esa.int (T.P.)

⁷ HeSpace, 64293 Darmstadt, Germany; Salvatore.Dinardo@eumetsat.int

* Correspondence: Pascal.Bonnefond@obspm.fr; Tel.: +33-1-4051-2229

Received: 20 November 2017; Accepted: 10 January 2018; Published: 11 January 2018

Abstract: Initially developed to monitor the performance of TOPEX/Poseidon and to follow the Jason legacy satellite altimeters at Senetosa Cape, Corsica, this calibration/validation site has been extended to include a new location at Ajaccio. This addition enables the site to monitor Envisat and ERS missions, CryoSat-2 and, more recently, the SARAL/AltiKa mission and Sentinel-3A satellites. Sentinel-3A and CryoSat-2 carry altimeters that use a synthetic aperture radar (SAR) mode that is different to the conventional pulse-bandwidth limited altimeters often termed “low resolution mode” (LRM). The aim of this study is to characterize the sea surface height (SSH) bias of the new SAR altimeter instruments and to demonstrate the improvement of data quality close to the coast. Moreover, some passes of Sentinel-3A and CryoSat-2 overfly both Senetosa and Ajaccio with only a few seconds time difference, allowing us to evaluate the reliability and homogeneity of both ground sites in term of geodetic datum. The Sentinel-3A and CryoSat-2 SSH biases for the SAR mode are respectively $+22 \pm 7$ mm and -73 ± 5 mm (for CryoSat-2 baseline C products). The results show that the stability of the SAR SSH bias time series is better than standard LRM altimetry. Moreover, compared to standard LRM data, for which the measurements closer than ~ 10 km from the coast were generally unusable, SAR mode altimeters provide measurements that are reliable at less than few hundred meters from the coast.

Keywords: altimetry; SAR; calibration; validation

1. Introduction

The Corsica geodetic facilities that are located both at Senetosa Cape for the TOPEX/Poseidon (T/P) and Jason satellite ground tracks and near Ajaccio for the Envisat satellite ground tracks have been developed to calibrate successive satellite altimeters in an absolute sense. Since 1998, the successful calibration process used to calibrate many oceanographic satellite altimeter missions has been regularly updated, see details in [1–3].

One of the main issues in comparing offshore altimetric sea surface height (SSH) measurements together with in-situ tide gauge data is taking into account the geoid slope (of several cm/km) over distances of tens of kilometers between both locations. As discussed in [4], other factors including ocean dynamics and tidal differences, impact the comparisons with independent coastal in situ measurements, but are negligible in such areas and within the short distance in our study (less than 20 km). A specific Global Positioning System (GPS) campaign was conducted in 1999 in order to determine a geoid map of about 20 km long and 5.4 km wide centered on the T/P and Jason satellite's ground track #085 at the Senetosa Cape site [4]. In addition, a second campaign was conducted in 2005 in the Ajaccio area under the Envisat ground track #130 (Figure 1) [5,6]. Both local geoids are the key datum for the absolute calibration of the satellite altimeters. Indeed, any distortion or systematic errors between offshore and tide gauge locations will cause a systematic error in the absolute SSH bias. From this point of view, the calibration process also requires accurate vertical offsets to be determined for each individual tide gauge in use. In order to achieve and maintain accuracy at the level of just a few millimeters or even less, geodetic campaigns must be carried out regularly in order to check or to eventually update such offsets.

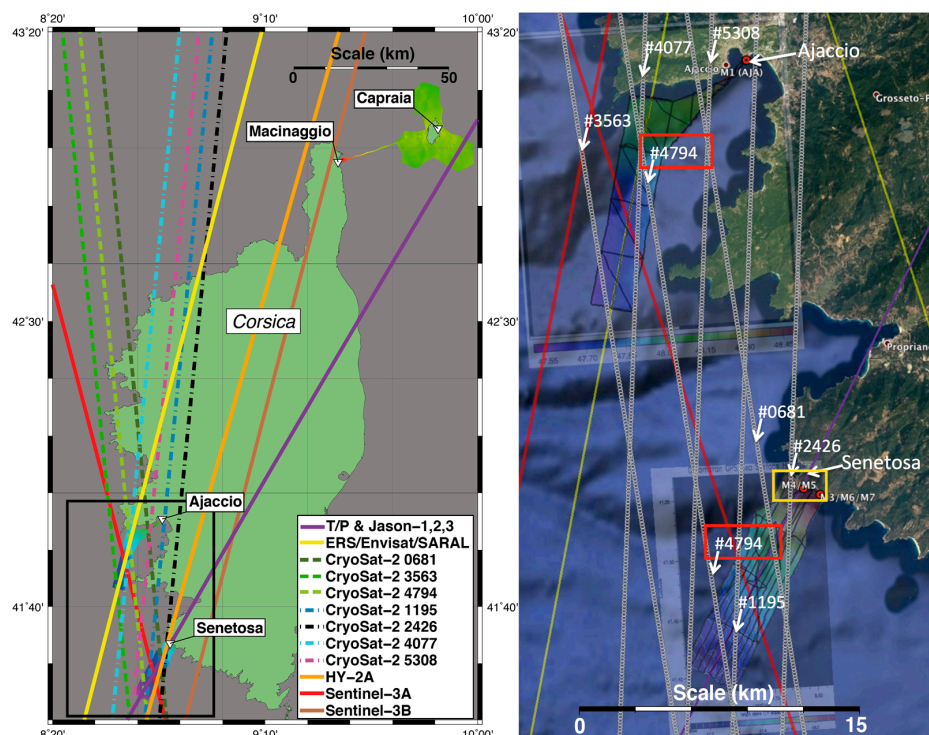


Figure 1. **Left:** General configuration of the Corsica calibration site with all of the satellite altimeter missions ground tracks that have been monitored since 1998 (the black frame on the left bottom corresponds to the zoom on the right map). **Right:** zoom on Ajaccio and Senetosa sites with Sentinel-3A (red) and CryoSat-2 (grey) tracks. The red rectangles highlight the CryoSat-2 pass #4794 that crosses the Senetosa and Ajaccio sites (see Section 0). The yellow rectangle shows the area that is discussed in Section 0 for pass #2426 (see Figure 8c).

The present paper focuses on the calibration of both the Sentinel-3A and CryoSat-2 missions using the same facilities and similar data processing. Sentinel-3A has a 27-day repeat cycle, where CryoSat-2 has a repeat cycle of 369 days and a 30-day sub-cycle; this repetition allows them to perform the absolute calibration over the Senetosa and Ajaccio area on a monthly basis for both satellites. Due to the configuration of Sentinel-3A repeat ground track and some CryoSat-2 passes, each altimeter overflies both the Senetosa and Ajaccio sites with a time delay of about five seconds corresponding

to a distance of about 37 km (Figure 1). As a consequence, it allows us to determine two SSH biases for each mission that should be equivalent considering that, most of the time, the sea state conditions at both sites are almost identical due to the short time delay and the short distance between sites. From the analysis of all available calibration passes, systematic differences can be related to errors in the geodetic references or in the situ data. For T/P-Jason and ERS-Envisat-SARAL/AltiKa this was difficult to determine as each altimeter mission overflowed only a single site, Senetosa or Ajaccio respectively. Since July 2016, the SARAL/AltiKa mission is in a drifting orbit phase allowing a similar study to the one presented here that is discussed in [7].

In this paper we first present the data and the methodology (Section 0). In the results section, Section 0, we present a re-processing of the Ajaccio tide gauge data following a re-analysis of the Global Positioning System (GPS) surveys that are used to monitor the location and any vertical movement of the tide gauges (Section 0). This resulted in an updated datum and a −30 mm vertical correction to the tide-gauge-derived SSH that is used in the calibration process of all the missions calibrated using the Ajaccio tide gauge data. The two following sections, 0 and 0, are then dedicated to the analysis of the Sentinel-3A [8] and CryoSat-2 [9] SSH biases, respectively.

2. Data and Methodology

2.1. Data

The data sets used for Sentinel-3 and CryoSat-2 are described below.

Sentinel-3A:

- Data sources: S3-PDGS (payload data ground segment) reprocessing 2017, Non-Time Critical (NTC) products: cycle 5–19, processing baseline 2.15 [10]. The processing baseline (PB) 2.15 consists of the following processors: SRAL L1 IPF V6.11, MWR L1 IPF V6.04, SRAL L2 IPF V6.07.
- Sentinel-3A SRAL (Ku/C Radar Altimeter) processing for SAR and Pseudo LRM (PLRM) and applied corrections
 - Standard processing: dual-frequency ionosphere measurement and wet troposphere radiometry. In this study, we also compared the dual frequency ionosphere measurements with the global ionosphere maps model (GIM), together with a comparison of the wet troposphere radiometer measurements with the wet troposphere model from European Centre for Medium-Range Weather Forecasts (ECMWF)). The chosen wet correction for the model corresponds to the field that is computed at sea level (MOD_WET_TROPO_COR_ZERO_ALTITUDE)
 - Dry troposphere
 - Sea state bias (SSB)
 - Solid, loading and pole tides
- In situ data
 - Ajaccio: Service Hydrographique et Océanographique de la Marine (SHOM) radar tide gauge data in real time
 - Senetosa: pressure tide gauges (data retrieved end of July 2017)

CryoSat-2:

- Data sources: from SARvatore service at ESA G-POD (https://gpod.eo.esa.int/services/CRYOSAT_SAR/) using baseline B products with two different retrackers. It is important to note that this product does not correspond to the current baseline C products processed by the CryoSat-2 payload data ground segment (PDGS), the main difference being the correction of a known range bias of 673 mm:

- SAMOSA2 retracker (default): The SAMOSA (SAR Altimetry MOde Studies and Applications) model [11] has been implemented in its first-order formulation (SAMOSA2) in a retracker as in [12]. This retracker uses a look-up table to mitigate the effect of the model's approximation of the squared PTR (point target response) with a Gaussian curve, it implements a stack masking for the Doppler beams padded to zero and has in principle no enhancement in the coastal zone.
- SAMOSA+ retracker (the SAMOSA2 model tailored for inland water, sea ice and the coastal zone domain): in the case of SAMOSA+, the open ocean SAMOSA [11] model and retracker [13] has been implemented in the retracking scheme with two significant additions [12]: The first one concerns the selection of the first-guess epoch. This is not selected as the position of the waveform peak but as the position of the moving correlation peak in 20 consecutive waveforms (after aligning them for tracker shift). The rationale behind this choice is to attempt to mitigate the typical off-ranging effect in coastal data. The second concerns the treatment of land-contaminated waveforms. In case waveforms are not contaminated by land, the SAMOSA model was used with the mean square slope set to zero, i.e., as in [13], whereas in the case of land contaminated waveforms, we used a dual step retracking: in the first step, the SWH is still estimated as in [13], while in the second step, the SWH was set to zero and the third free parameter in the retracking becomes the mean square slope. The output of this second step is the range and the amplitude P_u (retracked waveform amplitude, see Equation (22) in [12]).
- Cryosat-2 SIRAL (synthetic aperture interferometric radar altimeter) data processing for SAR and applied corrections
 - Dry troposphere
 - Wet troposphere from ECMWF model
 - Ionosphere from GIM
 - Sea state bias = 3.5% of SWH
 - Solid, loading and pole tides
- In situ data
 - Ajaccio: SHOM radar tide gauge data in real time
 - Senetosa: pressure tide gauges (data retrieved end of July 2017)

2.2. Methodology

The main difference in the processing in this study, compared to previous studies [1–3,6], is the difference in the footprint area in over which the geoid height is interpolated. In the case of LRM (low resolution mode, e.g., Jason missions), the footprint is defined as a circle using the significant wave height to define the diameter [14], while in the case of SAR (synthetic aperture radar, e.g., Sentinel-3A) the footprint is defined as a rectangle with a width of 300 m along-track and a length across-track that is also a function of SWH with the same formula as LRM (see Figure 5 or Figure 8 for an illustration).

Our standard processing of the SSH bias uses (when available) the wet tropospheric correction derived from the radiometer in addition to the ionospheric correction derived from the dual frequency of the altimeter. We performed a comparison with numerical weather prediction (NWP) model corrections that are available in the products for the wet troposphere and the ionosphere corrections, from ECMWF and GIM respectively (see Section 0).

3. Results

3.1. Solving the Vertical Offset in the Ajaccio Tide-Gauge-Derived SSH

In [3] we showed that there was an anomalous SSH bias of -30.5 ± 4.5 mm between the Ajaccio tide gauge and our GPS-based sea level measurements. We thus retrieved the GPS data from recent

surveys performed in 2013, 2014 and 2015 and computed new height differences between the antenna reference point (ARP) of the permanent receiver (AJAC) and the fundamental marker close to the tide gauge (G). This processing was done in baseline mode with the GAMIT software [15] and the results are shown in Table 1. The standard errors of the individual determinations range from 0.2 to 1.1 mm mainly due to the number of days of observation. It provides a much more coherent weighted mean value of 50.0371 m, rather than the 2005 reference, with a standard error of the weighted mean of 0.4 mm (Table 1), thus changing our historical reference by 18.3 mm.

Additionally, during the deployment of the Ajaccio tide gauge in 2012, the Service Hydrographique et Océanographique de la Marine (SHOM) performed SSH observations with a contact gauge and determined a 13.0 mm bias (standard deviation of 3.6 mm) which was introduced as a “calibration offset” into the tide gauge system. We decided to remove this quantity from the instrument and by adding it to the new correction (of 18.3 mm); the total systematic error of the tide gauge SHH has been established to be 31.4 mm. This is in very good agreement with the SSH bias observed between the Ajaccio tide gauge and our GPS-based sea level measurements (of -30.5 ± 4.5 mm [3]). We then changed our datum to a rounded offset of −30 mm in the tide gauge SSH. The results presented in this paper take this correction into account.

Another geodetic survey is planned for next year to confirm the height difference between the ARP of the permanent receiver (AJAC) and the fundamental marker close to the tide gauge (G), but we are already very confident in the current result given the 0.4 mm standard error.

Table 1. Height differences between permanent Global Positioning System (GPS) (AJAC) and tide gauge (G) at Ajaccio (in m).

Year	Reference Used	AJAC-G	Number of Days
2005	50.0188 ± 0.0100		
2013		50.0386 ± 0.0011	2
2014		50.0360 ± 0.0010	3
2015		50.0370 ± 0.0002	7
Average		50.0371 ± 0.0004	

3.2. Sentinel-3A SSH Calibration and Corrections Validation

The Sentinel-3A ascending pass #741 overflies the Senetosa site and ~5 s later the Ajaccio site. For the first time this allows us to compare the SSH biases, which can be independently determined at both locations, and then to assess geodetic references together with in-situ measurements. Launched on February 16th 2016, Sentinel-3A was in a ground-segment ramp-up phase during the first months with different versions of the IPF (instrument processing facilities) making the different cycles difficult to compare. Thanks to a reprocessing campaign [10] completed in September 2017 by the respective ESA and EUMETSAT agencies for cycles 5–19 (June 2016 to July 2017) with the same Processing Baseline 2.15, it is now possible to analyze a homogeneous set of data using the Non-Time Critical (NTC) product. We thus analyzed and compared the two modes which are used to derive the sea surface height from the radar measurements: (i) the SAR (synthetic aperture radar) mode and (ii) the PLRM (pseudo LRM) mode that mimics the classic LRM. A complete description of the products used and the processing options is given in Section 0.

Concerning the ionospheric correction, both the dual-frequency altimeter derived and the GIM model were averaged over a distance of ~140 km centered on the geoid area of Senetosa and Ajaccio (slightly shifted by ~14 km for Senetosa to avoid measurements over Sardinia). The results presented in Figure 2 show good consistency between the instrument and GIM model in terms of bias (+6 mm) and stability (5–6 mm). Moreover, the results from either the Senetosa or Ajaccio sites show good consistency.

Concerning the wet tropospheric correction deduced from the satellite radiometer, we have reduced the land contamination (as the radiometer has a large footprint) by filtering to keep the non-contaminated signal within our area of study. The selected corrections are linearly interpolated with an outlier rejection at 3σ up to the edges of the study area. They are then considered as a constant for both Senetosa and Ajaccio processing. The Senetosa interpolation area was used for

both the Senetosa and Ajaccio sites (Figure 3) because in this area the radiometer is almost not contaminated by land. The permanent GPS receiver at Senetosa and Ajaccio also allows us to compute the wet tropospheric corrections at these locations. Recently, Collecte Localisation Satellites (CLS) have developed an algorithm to reduce the land contamination in coastal conditions (available for cycle five to 15) [16]. The three wet tropospheric corrections were compared and the differences are shown in Figure 2. We note that the radiometer wet tropospheric correction provided in the products appears to be biased on average (Senetosa and Ajaccio) by -17.5 mm compared to the model and -20.5 mm compared to the GPS. The differences between the two sites are very small (3–5 mm). The ~ -20 mm bias is probably due to a remaining land contamination in the radiometer footprint. The analysis of the new radiometer correction developed by CLS to limit this effect shows better agreement with the correction derived from GPS. On the same time series (cycle 5–15), the bias is not only reduced by 15 mm in average but the standard deviation is also improved by 2 mm in average (Table 2).

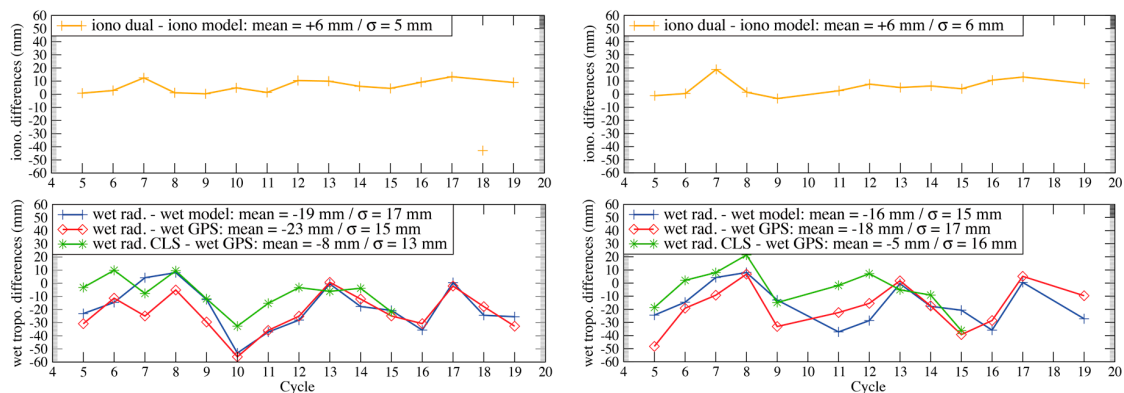


Figure 2. Sentinel-3A corrections differences at the Senetosa (**left**) and Ajaccio (**right**) calibration sites. Ionospheric correction differences in the upper panels. Wet tropospheric correction differences in the lower panels.



Figure 3. Map of the Sentinel-3A configuration: the shaded areas correspond to the locations where the wet tropospheric correction (radiometer and model) is interpolated.

A second study of the wet tropospheric correction was conducted using the Ajaccio interpolation area (Figure 3) that should be more sensitive to land contamination compared to Senetosa. All the other parameters are identical to the standard processing performed for Ajaccio. Figure 4 shows that, in this case, the wet tropospheric correction is biased by -79 mm (light blue) using the Ajaccio GPS wet tropospheric correction as a reference. The 59 mm increase in the difference between using the Ajaccio and Senetosa interpolation areas illustrates the challenge to fully remove land contamination in the radiometer footprint in such complex coastal areas. In this case, the CLS correction clearly provides a great improvement even though a residual bias of -14 mm still exists (orange). In addition, the differences between the wet tropospheric corrections deduced from both the Senetosa and Ajaccio GPS data (~ 37 km separation distance and only five seconds time lag for a typical satellite overpass) are given. It is worth noting that, if the corrections are equivalent ($+1$ mm) on average, the dispersion of 12 mm certainly reflects different meteorological conditions at both sites at the same time. We conclude and confirm that it is very important to use GPS measurements as close as possible to satellite radiometer data when computing wet tropospheric correction terms.

Table 2. Wet tropospheric correction differences on the common cycles (5–15) (in mm).

	Radiometer-GPS	
	Mean	σ
Senetosa		
Standard product	-23	16
CLS	-8	13
Ajaccio		
Standard product	-20	17
CLS	-5	16

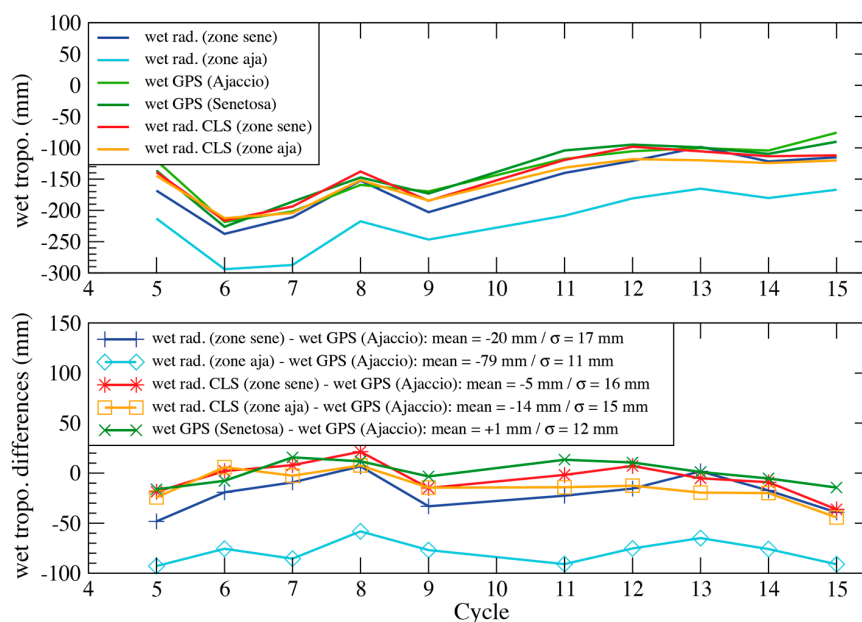


Figure 4. Sentinel-3A wet tropospheric correction differences at Ajaccio (using the Ajaccio interpolation area). Wet tropospheric correction in the upper panel: derived from satellite microwave radiometer using the Senetosa interpolation area (dark blue), radiometer using the Ajaccio interpolation area (light blue), GPS from Ajaccio (light green), GPS from Senetosa (dark green), radiometer (from Collecte Localisation Satellites (CLS)) using the Senetosa interpolation area (red) and radiometer (from CLS) using the Ajaccio interpolation area (orange). Wet tropospheric correction differences in the lower panel: reference is always the wet tropospheric correction from the Ajaccio GPS and same color code is used for the corrections being compared.

Finally, we also compared the corrections derived from the satellite instruments (radiometer and altimeter) using either SAR or PLRM processing. We found very small differences (<1 mm) that are caused by range differences between these two processing schemes. Finally, we compared the sea state bias corrections for SAR and PLRM that, for the moment, use the same correction tables: there are few millimeter differences originating from significant wave height (SWH) and wind speed differences, as the waveform shapes are different for SAR and PLRM.

The SSH calibration was performed independently at Ajaccio and Senetosa using respectively a radar tide gauge and three pressure tide gauges. Figure 5 illustrates the process used that is detailed in [3]. We recall that by convention the SSH bias corresponds to the difference ($\text{SSH}_{\text{altimetry}} - \text{SSH}_{\text{tide gauge}}$). This process was first carried out without taking into account the Ajaccio tide gauge SSH offset (see Section 0); a 26 mm offset clearly appears in the averaged results (-5 mm for Ajaccio and $+21$ mm for Senetosa) highlighting that the Ajaccio offset is clearly detectable by our absolute SSH calibration process. As a result, the Ajaccio tide gauge SSH time series were corrected by -30 mm, definitively. In Figure 5, the insert in green illustrates the improvement brought by SAR processed data. Indeed, when overflying the small Sanguinaires islands, only 2–3 data look bad and can be easily detected and rejected using a simple 3σ criteria (circled crosses). For comparison with LRM in the same area, all the Envisat data that were at a distance less than 10 km from the coast were eliminated [6]. However, it is important to note that the areas used to perform the calibration (blue boxes in Figure 5) are far enough (>10 km) to avoid any land contamination for the altimeter, except maybe in PLRM mode in the Ajaccio area.

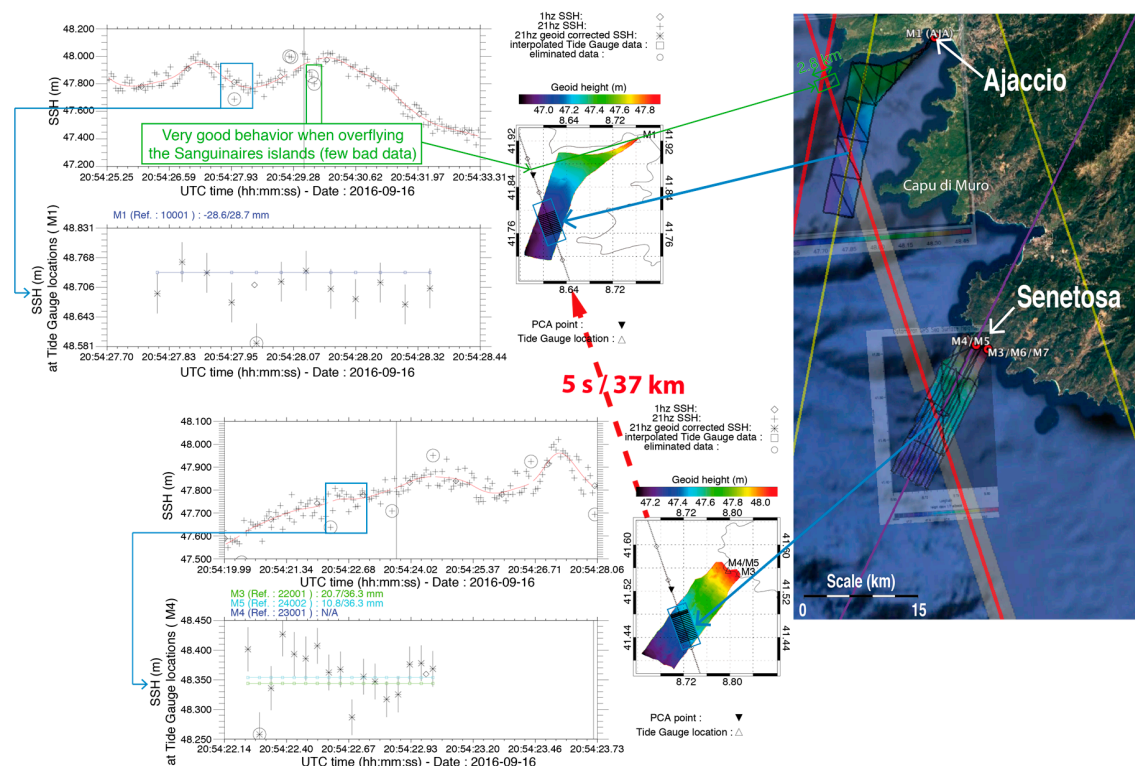


Figure 5. Example of sea surface height (SSH) bias processing for Sentinel-3A in synthetic aperture radar (SAR) mode (pass 741, cycle 8). For each independent processing (Ajaccio, top/Senetosa, bottom) the upper plot shows ± 4 s of altimeter SSH series around the point of closest approach (PCA). The lower plots show the selected SSH (inside the geoid area) that are corrected from the geoid height differences between the SSH location and the tide gauge locations.

The Figure 6 upper plots shows the SSH bias time series for SAR and PLRM respectively at Senetosa (left) and Ajaccio (right), while the lower plots show the differences (SAR-PLRM) either for “orbit-range” only or total SSH bias (“orbit-range + corrections”). The Ajaccio time series looks slightly noisier for SAR and much more so for PLRM compared to the Senetosa time series. This can be explained by more possible land contamination in the radar footprint in the Ajaccio area (e.g., the Capu di Muro and Sanguinaires islands, see Figure 5). The very good consistency of the “orbit-range” and “SSH bias” differences indicates that the correction differences between SAR and PLRM are very small, as explained previously. They are mainly due to SSB differences because SWH and wind speed estimations are different between SAR and PLRM processing. For the moment, the SSB model in the product is the same for SAR and PLRM. An improvement in terms of consistency is foreseen by the further tuning of SSB models for both SAR and PLRM, instead of using the same model. Thus, the main difference is due to range estimation that is different in SAR and PLRM processing.

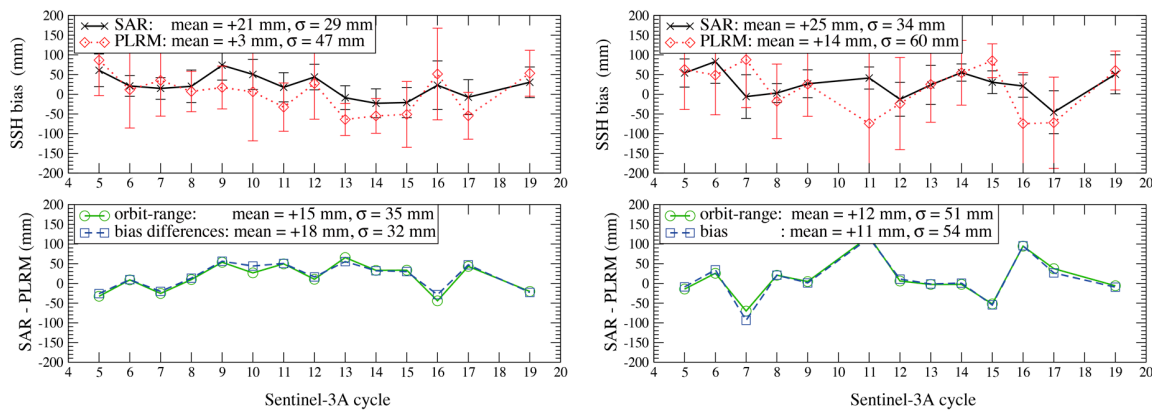


Figure 6. Sentinel-3A SSH bias time series from Senetosa (**left**) and Ajaccio (**right**). The upper panels show the time series for SAR (black crosses) and Pseudo LRM (PLRM) (red diamonds). The lower panels show the differences between SAR and PLRM for the “orbit-range” (green circles) and the total SSH bias (blue squares).

For each cycle, we have computed the averaged SSH bias from both Senetosa and Ajaccio independently (see the time series in Figure 7). First, it shows that the SSH bias for SAR is very stable with a standard deviation of 24 mm. Concerning the PLRM, as expected due to data processing issues (reconstruction of pseudo LRM waveforms from original SAR measurements that make the PLRM measurements noisier than real LRM), the standard deviation of 42 mm is higher than the classical LRM missions (e.g., 38 and 37 mm for Jason-1 and Jason-2 respectively [2]). Second, the 13 mm difference in the SSH bias between SAR and PLRM comes mainly from the differences in the altimeter range. From the entire data set (13 cycles), our best estimate of the SSH bias for Sentinel-3A is then:

- Sentinel-3A SAR: $+22 \pm 7$ mm
- Sentinel-3A PLRM: $+9 \pm 12$ mm

Recent studies using the transponder installed in Crete show that the SAR range bias is 0 ± 12 mm [17] and 8 ± 12 mm [18], so our results are in very good agreement because most of the SSH bias (+22 mm) originates from the radiometer wet tropospheric correction.

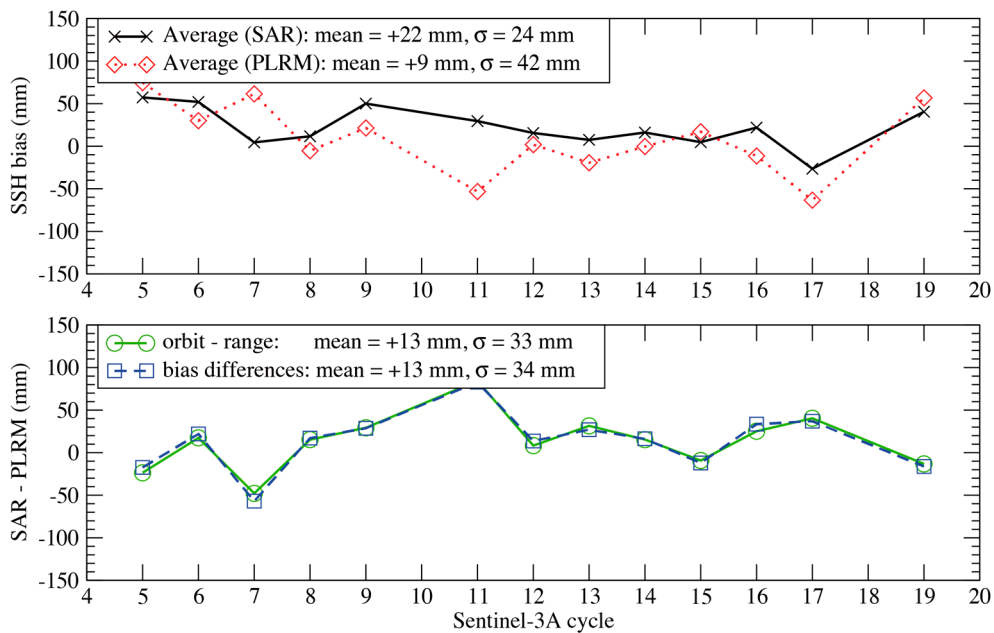


Figure 7. Average of Senetosa and Ajaccio Sentinel-3A SSH biases for both SAR and PLRM (upper panel). The lower panel shows the differences between SAR and PLRM for the “orbit-range” (green circles) and total SSH bias (blue squares).

3.3. CryoSat-2 SSH Calibration

Some of the CryoSat-2 altimeter passes overfly the Senetosa or Ajaccio facilities (or both). These passes are listed on Figure 1 (with their relative orbit number). In this study, we analyzed all these overflights with the same methodology as used for Sentinel-3A. In terms of our data set, we used the SARvatore service [19], which is part of the European Space Agency (ESA) grid processing on demand (G-POD) service. G-POD allows us to select an area and then process all of the L1a (FBR, full bit rate) data available to provide L2 products. It is possible to choose different options, but we have left all the options as default values. G-POD uses the SAMOSA2 retracker as default. However, another retracking approach tailored for coastal zones [11,12] was also available (SAMOSA+, SAR altimetry mode studies and applications) and we generated a separate set of data using this option. The different processing schemes were then used to analyze their impact on the SSH bias: SAMOSA2 for one set and SAMOSA+ for the other. The details on the data sets are given Section 0.

The configurations of the overflights are different from one CryoSat-2 ground track pattern to another (see Figure 1 right) but most of them have data very close to the coast (a few hundred meters, see Table 3). Descending pass #2426 is particularly interesting because the closest data is at ~1400 m from the M4/M5 tide gauges at Senetosa. Figure 8 illustrates the quality of the data for cycle 1 and the improvement for some data when using SAMOSA+ retracking. For the data before the point of closest approach (PCA), the SSH from SAMOSA+ decreases and appears more homogeneous with the rest of the time series (marked by green arrows in Figure 8a,b): one measurement at only 400 m across-track from the coast has been clearly improved even with about 37% of the footprint on land (marked by red arrows in Figure 8). However, most importantly, all the data immediately after the coastline (in time after the PCA, because it is a descending track) are of very good quality (marked by blue arrows in Figure 8) and do not look contaminated by land effects even with the classic SAMOSA2 retracker. This is clearly linked to the small area of the footprint for SAR in comparison with LRM. In this example, the footprint is a rectangle with a width of 300 m along-track and a length across-track of 3000 m (see white rectangle area in Figure 8c).

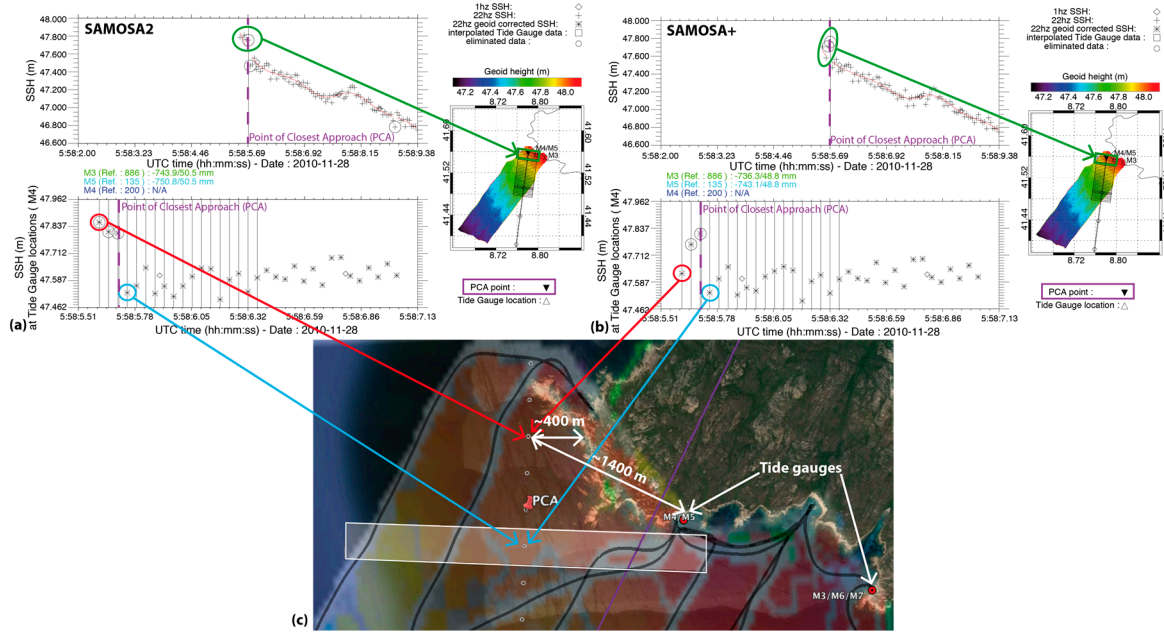


Figure 8. Example of retracking improvement for pass #2426 cycle 001. The upper panels of (a,b) show the altimeter SSH (crosses) without geoid correction, while the lower ones show the altimeter SSH after geoid correction (stars with error bars). An automatic outlier detection is performed and the rejected data are circled. (a) Corresponds to the G-POD standard retracking (SAMOSA2) while (b) corresponds to the improved retracking (SAMOSA+ is the SAMOSA2 model tailored for inland water, sea ice and coastal zone domains). (c) Shows a zoom of the data locations (circles) very close to the coast; the white rectangle represents the SAR footprint for one data; the black lines correspond to the Catamaran-GPS tracks [4] that were used to map the Senetosa geoid (colored map in background).

Table 3 provides the details of the SSH calibration for each pass and for the two retrackings used, and Figure 9 illustrates the time series of these SSH biases. Two passes in the Ajaccio area were not used because too few data were in the geoid area (#3563 and #5308, see Figure 1). The standard deviations of the individual mean SSH bias were respectively 14.6 mm and 14.0 mm for SAMOSA2 and SAMOSA+. This shows a small improvement for SAMOSA+, but if the same computation is done only for the “coastal” passes (#4077, #4794 and #2426), the standard deviations are this time respectively 15.2 mm and 12.5 mm. SAMOSA+ clearly improved the SSH when very close to the coast, avoiding some outliers even in the time series (see data circled in red in Figure 9 for pass #4794 at Ajaccio). The mean SSH bias for Senetosa and Ajaccio was -746 mm for both SAMOSA2 and SAMOSA+, but the overall standard deviation of the time series was improved by $\sim 13 \text{ mm}$ with SAMOSA+ ($\sqrt{(29^2 - 26^2)}$). The CryoSat-2 SSH bias is then:

- CryoSat-2 SAMOSA2: $-746 \pm 5.5 \text{ mm}$ ($-73 \pm 5.5 \text{ mm}$ for baseline C)
- CryoSat-2 SAMOSA+: $-746 \pm 5.0 \text{ mm}$ ($-73 \pm 5.0 \text{ mm}$ for baseline C)

We were unable to find in the literature another value of the CryoSat-2 absolute SSH bias (using sea level in situ measurements), but our results look very coherent with the updated Svalbard transponder result [20]: $722 \pm 6 \text{ mm}$ (standard deviation of 29 mm, baseline B, before correcting the 673 mm known range bias). It is worth noting that the 24 mm remaining difference between these two determinations can be due to the geophysical corrections, and notably that the SSB is not affecting the transponder processing.

For pass #4794, overflying both the Senetosa and Ajaccio facilities, we computed the averaged time series in the same way as for the Sentinel-3A pass shown in Figure 7. This is presented in Figure 10, where the average SSH bias from the Ajaccio and Senetosa overflights (5 s time lag and 37 km distance)

showed a very low standard deviation (15 mm for SAMOSA+ and 17 mm for SAMOSA2) and a bias very close to the global average: -740 mm for SAMOSA+ and -741 mm for SAMOSA2 vs. -746 mm for the global average (for both SAMOSA+ and SAMOSA2). For comparison, with a similar configuration, the standard deviation over 13 cycles for Sentinel-3A was 24 mm.

Table 3. Details of the SSH biases for each pass and for the two retrackers (SAMOSA2 and SAMOSA+).

Passes	SAMOSA2			SAMOSA+			Comment
	Mean (mm)	σ (mm)	Number of Cycles	Mean (mm)	σ (mm)	Number of Cycles	
Ajaccio							
3563	NA	NA	NA	NA	NA	NA	Coastal *
4077	-746	32	5	-743	30	5	Coastal *
4794	-727	36	5	-731	24	5	Coastal *
5308	NA	NA	NA	NA	NA	NA	Coastal *
Average	-736	33	10	-737	26	10	
Senetosa							
0681	-766	17	5	-768	14	4	
1195	-733	23	3	-733	23	3	$d > 8$ km
2426	-757	36	4	-756	35	4	Coastal *
4794	-742	26	6	-746	23	6	$d > 13$ km
Average	-751	27	18	-751	26	17	
Total	-746	29	28	-746	26	27	

* Coastal means that we take the measurements up to the coast; for the others the distance “d” is the closest measurement to the coast.

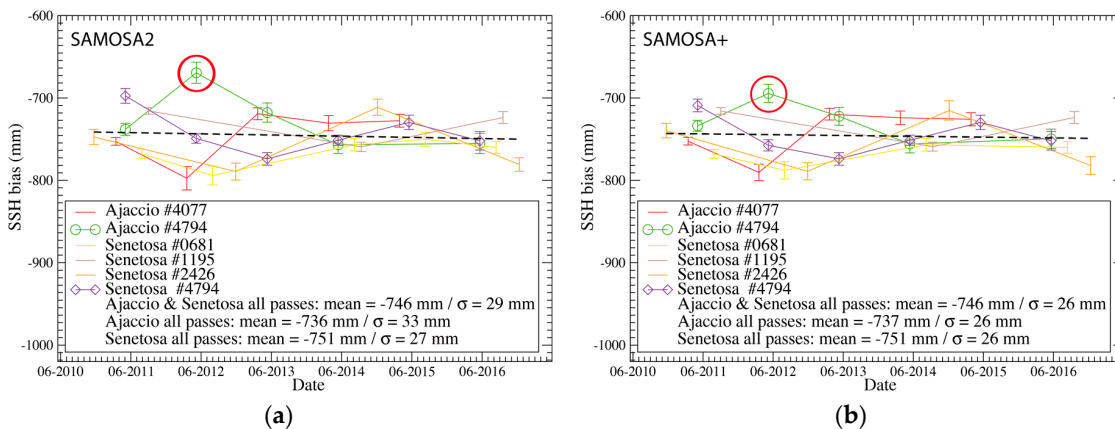


Figure 9. Time series of the CryoSat-2 SSH biases for each pass and the averages from Ajaccio, Senetosa and both (dash black line): (a) corresponds to the G-POD standard retracking (SAMOSA2) while (b) corresponds to the improved retracking (SAMOSA+) tuned for coastal, inland waters and ice.

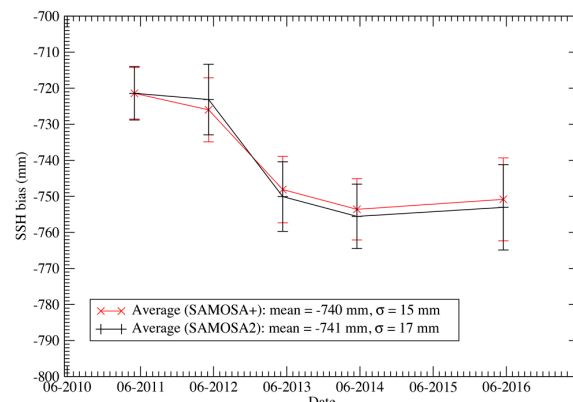


Figure 10. Example of pass #4794 with a configuration « à la » Sentinel-3A from which the SSH biases from Ajaccio and Senetosa were averaged (using SAMOSA+).

4. Discussion and Conclusions

The configuration of the Sentinel-3A and CryoSat-2 passes allowed us to cross-compare the results obtained independently from both the Senetosa and Ajaccio sites. Our results confirm previous results that were obtained from SARAL/AltiKa together with GPS-based sea level measurements [3]. The SSH measured by the Ajaccio tide gauge is biased by ~30 mm and our present study shows the origin of this offset. By taking into account this offset, we compared results from the Senetosa and Ajaccio sites for both the Sentinel-3A and CryoSat-2 altimeters. For the Sentinel-3A the site-difference between Senetosa and Ajaccio was −4 mm (21–25 mm, see Figure 6) while for CryoSat-2 the difference was −14 mm ((−751)−(−737) mm, see Figure 9 from SAMOSA+ results). These comparisons show that no significant systematic error remains in the geodetic datum or in situ measurements. This is a very important result that gives us confidence also for the historical calibrations performed independently at each site. However, differences still exist at the millimeter level between the SSH bias obtained at the Senetosa and Ajaccio sites for Sentinel-3A and CryoSat-2 (respectively −4 and −14 mm). This probably reflects some remaining errors in the altimeter measurement system (coastal contamination, sea state bias, . . .) and/or in the local geodetic datum of both the Senetosa and Ajaccio sites. Finally, our analysis of the wet tropospheric corrections available for the Sentinel-3A calibration showed that the effect of land contamination on the radiometer was ∼−20 mm, which is actually the main part of the SSH bias (+22 ± 7 mm). In terms of the range itself, we can consider that SAR measurement system on Sentinel-3A as “unbiased”. For CryoSat-2, it is important to recall that the product used from G-POD is based on baseline B, so to be comparable to the current baseline C, one must remove the known range bias of 673 mm to the SSH biases determined in this study: when using baseline C products, the CryoSat-2 SSH bias is -73 ± 5 mm. Last but not least, the SSH biases for both Sentinel-3A and CryoSat-2 were compared to the range biases determined with transponders located respectively in Crete and Svalbard, and the remaining differences (respectively 22 mm and 24 mm) between these two determinations can be due to geodetic datum errors or geophysical corrections and, notably, the sea state bias that is not affecting transponder processing. This is probably the first time in altimetry that the results from transponders and in situ SSH calibration agree at this level of accuracy.

Acknowledgments: This study was conducted and financed thanks to Centre National d’Etudes Spatiales (CNES), Centre National de la Recherche Scientifique (CNRS), and the French Ministry of Research.

Author Contributions: Pascal Bonnefond and Olivier Laurain designed the study, analyzed the data and wrote the paper. All the other co-authors helped in paper writing and analysis.

Conflicts of Interest: The authors declare no conflict of interest.

References

1. Bonnefond, P.; Exertier, P.; Laurain, O.; Menard, Y.; Orsoni, A.; Jan, G.; Jeansou, E. Absolute Calibration of Jason-1 and TOPEX/Poseidon Altimeters in Corsica Special Issue on Jason-1 Calibration/Validation. *Mar. Geod.* **2003**, *26*, 261–284. [[CrossRef](#)]
2. Bonnefond, P.; Exertier, P.; Laurain, O.; Jan, G. Absolute Calibration of Jason-1 and Jason-2 Altimeters in Corsica during the Formation Flight Phase. *Mar. Geodesy* **2010**, *33*, 80–90. [[CrossRef](#)]
3. Bonnefond, P.; Laurain, O.; Exertier, P.; Guillot, A.; Picot, N.; Cancet, M.; Lyard, F. SARAL/AltiKa absolute calibration from the multi-mission Corsica facilities. *Mar. Geodesy* **2015**, *38*, 171–192. [[CrossRef](#)]
4. Bonnefond, P.; Haines, B.; Watson, C. In Situ Calibration and Validation: A Link from Coastal to Open-ocean altimetry, chapter 11. In *Coastal Altimetry*; Vignudelli, S., Kostianoy, A., Cipollini, P., Benveniste, J., Eds.; Springer: Berlin/Heidelberg, Germany, 2011; pp. 259–296. ISBN 978-3-642-12795-3.
5. Bonnefond, P.; Exertier, P.; Laurain, O.; Menard, Y.; Orsoni, A.; Jeansou, E.; Haines, B.; Kubitschek, D.; Born, G. Leveling Sea Surface using a GPS catamaran. *Mar. Geodesy* **2003**, *26*, 319–334. [[CrossRef](#)]
6. Bonnefond, P.; Exertier, P.; Laurain, O.; Lyard, F.; Bijac, S.; Cancet, M.; Chimot, J.; Féminias, P. Corsica: An experiment for long-term Altimeter calibration and sea level monitoring. In Proceedings of the ESA Living Planet Symposium, Bergen, Norway, 28 June–2 July 2010.

7. Bonnefond, P.; Verron, J.; Babu, K.N.; Bergé-Nguyen, M.; Cancet, M.; Chaudhary, A.; Crétaux, J.F.; Frappart, F.; Haines, B.J.; Laurain, O.; et al. The Benefits of the Ka-Band as Evidenced from the SARAL/AltiKa Altimetric Mission: Quality Assessment and Unique Characteristics of AltiKa Data. *Remote Sens.* **2017**, *10*, 83. [[CrossRef](#)]
8. Donlon, C.; Berruti, B.; Buongiorno, A.; Ferreira, M.-H.; Féménias, P.; Frericka, J.; Goryl, P.; Kleina, U.; Laur, H.; Mavrocordatos, C.; et al. The Global Monitoring for Environment and Security (GMES) Sentinel-3 mission. *Remote Sens. Environ.* **2012**, *120*, 37–57. [[CrossRef](#)]
9. Bouffard, J.; Webb, E.; Scagliola, M.; Garcia-Mondéjar, A.; Baker, S.; Brockley, D.; Gaudelli, J.; Muir, A.; Hall, A.; Mannan, R.; et al. CryoSat Instrument Performance and Ice Product Quality Status. *Adv. Space Res.* **2017**. [[CrossRef](#)]
10. Sentinel-3A SRAL Reprocessed Dataset Available on CODA from 16 October. Available online: https://www.eumetsat.int/website/home/News/DAT_3648215.html (accessed on 6 November 2017).
11. Ray, C.; Martin-Puig, C.; Clarizia, M.P.; Ruffini, G.; Dinardo, S.; Gommenginger, C.; Benveniste, J. SAR altimeter backscattered waveform model. *IEEE Trans. Geosci. Remote Sens.* **2015**, *53*, 911–919. [[CrossRef](#)]
12. Dinardo, S.; Fenoglio-Marc, L.; Buchhaupt, C.; Becker, M.; Scharroo, R.; Fernandez, J.M.; Benveniste, J. Coastal SAR and PLRM Altimetry in German Bight and West Baltic Sea. *Adv. Space Res.* **2017**, in press. [[CrossRef](#)]
13. Fenoglio-Marc, L.; Dinardo, S.; Scharroo, R.; Roland, A.; Dutour Sikiric, M.; Lucas, B.; Becker, M.; Benveniste, J.; Weiss, R. The German Bight: A validation of CryoSat-2 altimeter data in SAR mode. *Adv. Space Res.* **2015**, *55*, 2641–2656. [[CrossRef](#)]
14. Chelton, D.B.; Walsh, E.J.; MacArthur, J.L. Pulse compression and sea level tracking in satellite altimetry. *J. Atmos. Ocean. Technol.* **1989**, *6*, 407–428. [[CrossRef](#)]
15. King, R.; Bock, Y. Documentation for the GAMIT GPS Analysis Software. Release 10, Massachusetts Institute of Technology, Cambridge. 2000. Available online: <http://www-gpsg.mit.edu/~simon/gtgk/GAMIT.pdf> (accessed on 5 October 2017).
16. Picard, B.; Fréy, M.; Pardé, M.; Bonnefond, P.; Laurain, O.; Crétaux, J.-F. A Wet Tropospheric Correction Dedicated to Hydrological and Coastal Applications. In Proceedings of the Ocean Surface Topography Science Team Meeting, Miami, FL, USA, 23–27 October 2017; Available online: https://meetings.aviso.altimetry.fr/fileadmin/user_upload/tx_ausyclsseminar/files/OSTST-2017_PICARD_NewCoastalNN_POSTER.pdf (accessed on 6 November 2017).
17. Mertikas, S.; Donlon, C.; Mavrocordatos, C.; Féménias, P.; Galanakis, D.; Tziavos, I.; Boy, F.; Vergos, G.; Andersen, O.; Frantzis, X.; et al. Multi-mission calibrations results at the Permanent Facility for Altimetry Calibration in west Crete, Greece attaining Fiducial Reference Measurement Standards. In Proceedings of the Ocean Surface Topography Science Team Meeting, Miami, FL, USA, 23–27 October 2017; Available online: https://meetings.aviso.altimetry.fr/fileadmin/user_upload/tx_ausyclsseminar/files/OSTST_CalVal_20_Oct_2017_Mertikas_AAA.pdf (accessed on 6 November 2017).
18. Garcia-Mondejar, A.; Mertikas, S.; Galanakis, D.; Labroue, S.; Bruniquel, J.; Quartly, G.; Féménias, P.; Mavrocordatos, C.; Wood, J.; Garcia, G.; et al. Sentinel-3 Transponder Calibration Results. In Proceedings of the Ocean Surface Topography Science Team Meeting, Miami, FL, USA, 23–27 October 2017; Available online: https://meetings.aviso.altimetry.fr/fileadmin/user_upload/tx_ausyclsseminar/files/S3 OSTST Poster_20171012_V8.pdf (accessed on 6 November 2017).
19. Dinardo, S. Guidelines for the SAR (Delay-Doppler) L1b Processing. 2013. Available online: http://wiki.services.eoportal.org/tiki-download_wiki_attachment.php?attId=2540 (accessed on 5 October 2017).
20. Garcia-Mondejar, A.; Fornari, M.; Bouffard, J.; Féménias, P.; Roca, M. CryoSat-2: Range, Datation and Interferometer Calibration with Svalbard Transponder. *Adv. Space Res.* **2017**, under review.



© 2018 by the authors. Licensee MDPI, Basel, Switzerland. This article is an open access article distributed under the terms and conditions of the Creative Commons Attribution (CC BY) license (<http://creativecommons.org/licenses/by/4.0/>).